J. Phys. B: At. Mol. Opt. Phys. 22 (1989) 83-97. Printed in the UK

Partial and state-selective cross sections for multiple ionisation of rare-gas atoms by electron impact

H Lebius, J Binder, H R Koslowski, K Wiesemann and B A Huber
Institut für Experimentalphysik AG II, Ruhr-Universität Bochum, D-4630 Bochum, Federal Republic of Germany

Received 22 July 1988

Abstract. Partial ionisation cross sections for single electron impact on rare-gas atoms (Ne, Kr and Xe) have been measured for charge states up to $q=8$. In addition, by using the translational energy spectroscopy technique (TES) we have determined state-selective cross sections for the production of doubly and triply charged neon ions in specific electronic states. The contributions of direct and inner-shell processes are discussed.

1. Introduction

The partial ionisation of neutral atoms is described by the following equation:

$$e^- + A \rightarrow A^{q+} + (q+1)e^-.$$

The cross section for this reaction is called the partial cross section and is designated by σ_q. The gross ionisation cross section σ is defined as the sum of partial cross sections weighted by the corresponding charge state:

$$\sigma = \sum_q q\sigma_q.$$

Measurements of gross and partial cross sections for low charge states have been performed by several groups, but there are only a few data available for the production of highly charged ions in the electron energy range from threshold up to 1 keV.

The measurement of these cross sections is very important for various applications as the values differ significantly from results of the Bethe–Born approximation in the energy range considered. Furthermore, in order to study the selective population of electronically excited levels, e.g. in connection with the development of new laser schemes or the modelling of laboratory or astrophysical plasmas, state-selective cross sections have to be determined as well. At present, the corresponding data are rather scarce. We have extended our earlier measurements in argon (Wiesemann *et al* 1987, Huber 1987) to the rare gases neon, krypton and xenon.

2. Experimental set-up

The experimental arrangement and the procedure of measurement are described in detail elsewhere (Koslowski *et al* 1987, Wiesemann *et al* 1987). Briefly, multiply charged ions are produced in an electron impact ion source under single collision

0953-4075/89/010083+15$02.50

conditions; they are extracted and analysed with respect to their charge state by a magnetic sector field. The ions pass through a collision chamber and an energy analyser which may be used for the purpose of TES before being detected with the aid of a channeltron. The extraction, transmission and detection efficiencies are determined by comparing the counting rate of singly charged ions with well established single ionisation cross sections versus electron energy. In addition, our relative cross sections are normalised at one electron energy with respect to absolute values as measured by other authors. The error made by this correction and normalisation is about 5-10% plus the uncertainty of the data point used for normalisation.

3. Partial ionisation cross sections

We have measured partial cross sections for the production of multiply charged ions of neon ($q=2$-4), krypton ($q=2$-8) and xenon ($q=2$-5), which are shown in figures 1-3. The corresponding values are listed in tables 1-3.

Total cross sections from Rapp and Englander-Golden (1965), which have been corrected for twice the double ionisation cross section as measured by several authors

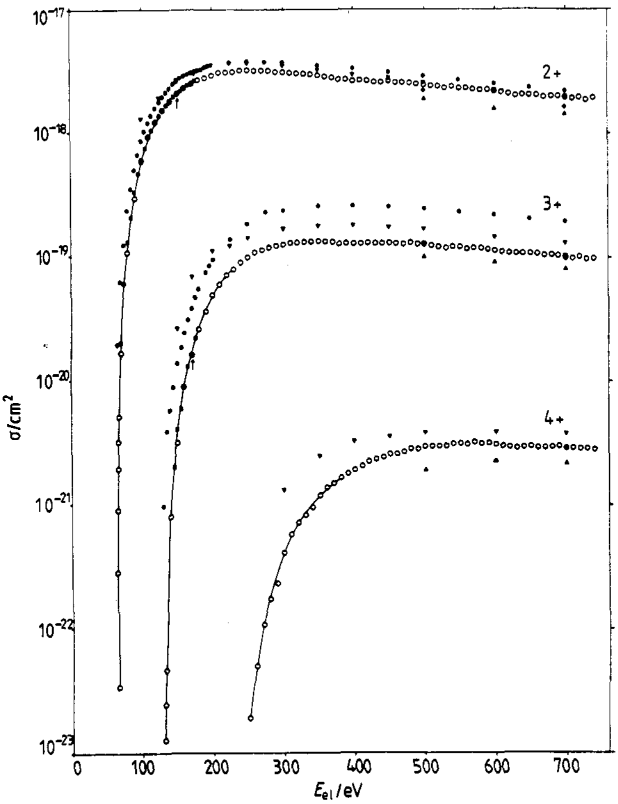

Figure 1. Cross sections for double, triple and quadruple ionisation of neon. The arrows indicate the points of absolute normalisation. The lines are shown to guide the eye only. ○, our results; ■, Stephan *et al* (1980); ◆, Nagy *et al* (1980); ▲, Schram *et al* (1966); ▼, Gaudin and Hagemann (1967); ●, Krishnakumar and Srivastava (1988).

Table 1. Partial ionisation cross sections for electron impact on neon for electron energies from threshold up to 750 eV.

E_{el}/eV	$\sigma^{2+}/10^{-18}$ cm^2	$\sigma^{3+}/10^{-19}$ cm^2	$\sigma^{4+}/10^{-21}$ cm^2
63	0.000 034		
64	0.000 289		
65	0.000 918		
66	0.001 97		
67	0.003 26		
68	0.005 27		
70	0.017 0		
80	0.122		
90	0.300		
100	0.584		
110	0.923		
120	1.21		
127		0.000 00444	
128		0.000 0165	
129		0.000 0488	
130	1.52	0.000 127	
131		0.000 243	
132		0.000 472	
140	1.77	0.008 09	
150	2.08	0.032 1	
160	2.30	0.088 6	
170	2.51	0.160	
180	2.71	0.261	
190	2.85	0.374	
200	2.99	0.501	
210	3.13	0.614	
220	3.18	0.733	
230	3.19	0.809	
240	3.26	0.915	0.001 32
250	3.27	1.00	0.018 4
260	3.25	1.10	0.050 4
270	3.26	1.15	0.109
280	3.24	1.20	0.175
290	3.20	1.24	0.238
300	3.20	1.27	0.419
310	3.14	1.32	0.594
320	3.14	1.33	0.730
330	3.12	1.35	0.847
340	3.07	1.36	0.978
350	3.00	1.37	1.22
360	2.92	1.36	1.41
370	2.90	1.34	1.53
380	2.78	1.30	1.70
390	2.77	1.31	1.84
400	2.71	1.31	1.97
410	2.73	1.31	2.11
420	2.70	1.32	2.29
430	2.65	1.31	2.39
440	2.64	1.31	2.49
450	2.71	1.32	2.62
460	2.62	1.31	2.63
470	2.62	1.29	2.72
480	2.59	1.33	2.89

Table 1. (continued)

E_{el}/eV	$\sigma^{2+}/10^{-18}$ cm^2	$\sigma^{3+}/10^{-19}$ cm^2	$\sigma^{4+}/10^{-21}$ cm^2
490	2.53	1.29	2.86
500	2.53	1.29	3.01
510	2.47	1.26	3.04
520	2.45	1.23	3.01
530	2.39	1.20	3.03
540	2.43	1.23	3.17
550	2.38	1.22	3.20
560	2.35	1.29	3.15
570	2.32	1.20	3.27
580	2.29	1.19	3.17
590	2.29	1.17	3.24
600	2.22	1.15	3.14
610	2.19	1.12	3.04
620	2.12	1.10	2.97
630	2.05	1.09	2.93
640	2.08	1.09	2.99
650	2.07	1.09	3.01
660	2.05	1.08	2.96
670	1.98	1.05	2.96
680	2.01	1.06	2.97
690	2.01	1.04	3.00
700	1.99	1.03	2.90
710	1.95	0.98	2.90
720	1.98	1.01	2.86
730	1.89	0.97	2.86
740	1.95	0.98	2.83
750	1.90	0.98	2.79

(Stephan *et al* 1980, Stephan and Märk 1984, Schram *et al* 1966, Schram 1966), have been used in order to derive the correction function for higher charge states (for details see Wiesemann *et al* 1987). For $q = 2$ and 3 an absolute calibration has been obtained by comparing our data with recommended values of Stephan *et al* (1980) or Stephan and Märk (1984) at an electron energy close to 150 eV. For higher charge states the cross sections have been normalised at higher electron energies, the only energy range where results from other authors are available. However, in some cases these data sets deviate by a factor of about 2. Considering the agreement between the corresponding low-charge state data we have selected the most probable value or have chosen an arithmetic average for the normalisation of our data.

The total errors in the cross sections contain the statistical errors as well as the uncertainty of the cross section values used for an absolute calibration. These errors are 10% for Ne^{2+}, Kr^{2+}–Kr^{4+} and Xe^{2+}, (10–20)% for Kr^{5+}, Kr^{6+} and Xe^{3+}, (20–30)% for Ne^{3+}, Ne^{4+}, Kr^{7+}, Xe^{4+} and Xe^{5+} and 50% for Kr^{8+}. For cross sections lower than 10^{-22} cm^2 the errors are about (50–80)%.

The ionisation curves of neon are rather smooth, showing no structure due to inner-shell contributions. This is understandable, as the energy which is required to remove a 1s electron in neon amounts to 870 eV and thus lies beyond the measured

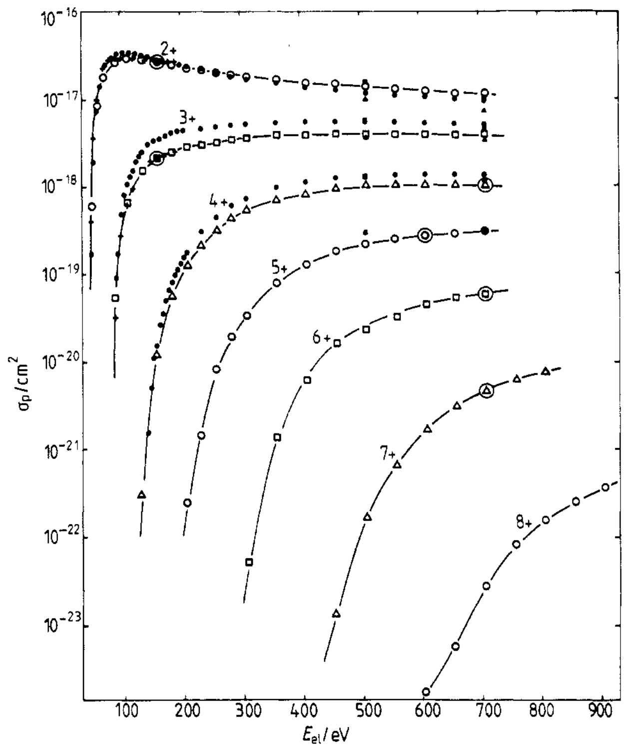

Figure 2. Partial ionisation cross sections for the production of Kr^{2+} up to Kr^{8+}. Open symbols indicate our data, the cross sections are normalised at the points marked with a cricle. The lines only guide the eye. +, Stephan *et al* (1980); ▲, Nagy *et al* (1980); ■, Schram (1966); ●, Krishnakumar and Srivastava (1988).

energy domain. Whereas for Ne^{2+} the agreement with results of other authors is quite satisfying, in Ne^{3+} the situation is different. At high electron energies the results of Gaudin and Hagemann (1967) and Krishnakumar and Srivastava (1988) clearly exceed our cross sections and the data obtained by Schram *et al* (1966) are somewhat lower than the present ones. This general tendency, which is also found in other systems, is not understood at present. Due to this behaviour cross sections for Ne^{4+} have been normalised with respect to the arithmetic average of the available data at high energies.

Figure 2 shows partial ionisation cross sections for the production of Kr ions in charge states 2–8. In contrast to our results in Ar these curves are rather smooth for all charge states. Only the curve for triple ionisation shows some structure close to $E_{el} = 220$ eV, which corresponds to the binding energy of a 3p electron. For $q = 2$ inner-shell contributions seem to be negligible, whereas for higher charge states ($q > 4$) the minimal ionisation energy lies close to or even above the binding energy of inner electrons. Therefore inner-shell contributions will not show up in the course of the ionisation function although these processes are supposed to dominate the ionisation process as we have shown in the case of Ar (Koslowski *et al* 1987).

The double ionisation cross section of xenon rises significantly at an electron energy of about 68 eV which is the binding energy of a 4d electron in xenon (see figure 3). The emission of a 4d electron is followed by the Auger process $N_{4,5}O_{2,3}O_{2,3}$ leading to a doubly charged xenon ion. Contributions from further inner subshells (4p, 4s

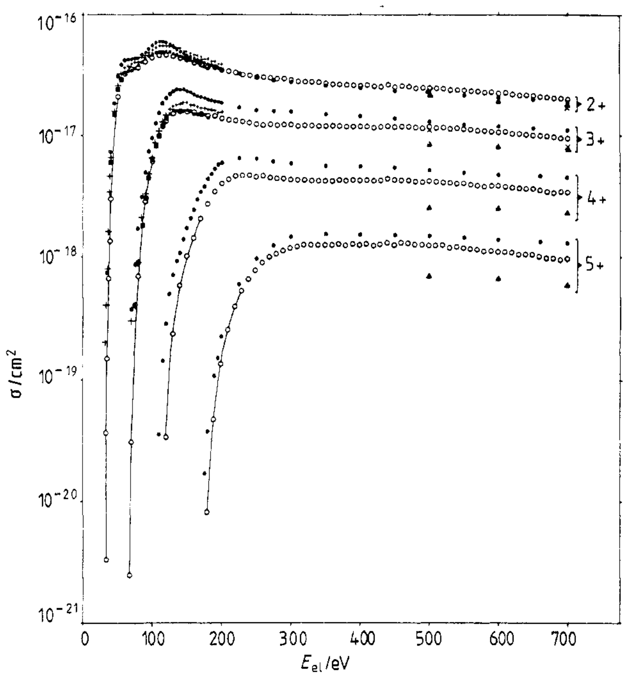

Figure 3. Measured cross sections for the production of Xe^{2+} up to Xe^{5+}. The lines only guide the eye. ○, our results; ■, Stephan and Märk (1984); ×, Nagy *et al* (1980); ▲, Schram (1966); ●, Krishnakumar and Srivastava (1988); +, Wetzel *et al* (1987).

with threshold values of 150 eV and 215 eV, respectively) are not clearly reflected in the course of the cross sections. A comparison with results of different authors yields good agreement for Xe^{2+}; however, the deviations become larger with increasing charge state of the product ion. In the case of Xe^{4+} and Xe^{5+} an absolute comparison seems to be less meaningful as our data have been normalised to an arithmetic average value at higher electron energies.

Concerning the relative shape of the ionisation functions there are deviations larger than the error bounds given by different authors which are of the order of (5–10)%. For example, the ratio of the relative cross section values measured by us and Krishnakumar and Srivastava (1988) changes for the fourfold ionisation of Xe from 3 to 1.3 when the electron energy is increased from 130 eV to 700 eV. The reason for this discrepancy is not understood up to now.

4. State-selective ionisation cross sections

By applying translational energy spectroscopy we have measured the composition of the ion beams with respect to the ground state and the two low-lying metastable states. By multiplying the partial ionisation cross sections by the relative beam fractions state-selective cross sections are obtained. As the time of flight of the ions from production to detection is about 10 μs we can only detect ions in the ground state and

Table 2. Partial ionisation cross sections for the electron impact on krypton for electron energies from threshold up to 900 eV.

E / eV	σ^{2+} / 10^{-17} cm^2	σ^{3+} / 10^{-18} cm^2	σ^{4+} / 10^{-19} cm^2	σ^{5+} / 10^{-19} cm^2	σ^{6+} / 10^{-20} cm^2	σ^{7+} / 10^{-21} cm^2	σ^{8+} / 10^{-22} cm^2
40	0.061						
50	0.88						
60	1.84						
80	2.78	0.054					
100	3.10	0.67					
125	2.97	1.54					
130			0.0031				
150	2.81	2.21	0.12				
175	2.58	2.55	0.56				
200	2.35	2.95	1.27	0.0025			
225	2.23	3.09	2.14	0.014			
250	2.10	3.31	3.25	0.084			
275	2.00	3.53	4.48	0.12			
300	1.88	3.65	5.45	0.34	0.005		
350	1.72	3.92	7.25	0.80	0.13		
400	1.59	3.91	8.26	1.29	0.63		
450	1.51	3.98	9.59	1.82	1.60	0.013	
500	1.44	4.02	10.4	2.20	2.26	0.15	
550	1.33	3.96	10.6	2.51	3.18	0.62	0.008
600	1.26	3.99	10.5	2.78	4.29	1.54	0.015
650	1.18	3.83	10.4	2.91	5.06	2.96	0.05
700	1.19	3.98	10.3	3.10	5.56	4.34	0.26
750						5.87	0.75
800						7.13	1.4
850							2.3
900							3.4

in metastable states. Other electronic states decay into these long-lived states and therefore the given state-selective cross sections contain cascade contributions from higher states. However, as seen for the double ionisation of Ar (Wiesemann *et al* 1987) the state-selective ionisation cross sections decrease rapidly with increasing excitation energy; thus cascade contributions to low-lying states are believed to be rather small.

In the case of Ne^{2+}, beam fractions have been determined by analysing the translational energy spectra of Ne^{+} ions produced in Ne^{2+}/Xe collisions. For different spectra the electron energy has been varied in the ion source (for the analysis of the spectrum see e.g. Huber and Kahlert (1984)). The intensity of a specific reaction channel is proportional to the cross section and the current of incident projectile ions in the corresponding state. The proportional constants, i.e. the cross sections, are obtained by absolute measurement of the beam fractions at one electron energy. For this purpose the translational attenuation method (TAM) has been applied and collisional excitation and de-excitation spectra have been interpreted and evaluated (Kobayashi *et al* 1983).

For the TAM we use an additional collision chamber where the ion beam is attenuated by a static gas target. This method can be applied if the attenuation cross section depends strongly on the internal state of the ion. Depending on the size of the cross

Table 3. Partial ionisation cross sections for the production of Xe^{2+} up to Xe^{5+} for electron energies from threshold to 700 eV.

E_{el}/eV	$\sigma^{2+}/10^{-17}$ cm^2	$\sigma^{3+}/10^{-17}$ cm^2	$\sigma^{4+}/10^{-18}$ cm^2	$\sigma^{5+}/10^{-19}$ cm^2
33.4	0.000 433			
34	0.003 68			
35	0.014 5			
37	0.067 1			
39	0.135			
40	0.297			
50	2.09			
60	3.25			
68		0.000 254		
69		0.001 38		
70	3.54	0.003 20		
80	3.65	0.070 2		
90	4.07	0.285		
100	4.37	0.606		
110	4.64	1.00		
120	4.65	1.32	0.0391	
130	4.57	1.52	0.239	
140	4.39	1.60	0.594	
150	4.24	1.58	1.03	
160	4.00	1.56	1.45	
170	3.9	1.5	2.08	
180	3.73	1.46	2.76	0.0807
190	3.67	1.45	3.52	0.469
200	3.51	1.39	4.08	1.34
210	3.41	1.36	4.43	2.52
220	3.34	1.33	4.69	3.91
230	3.21	1.31	4.79	5.29
240	3.16	1.29	4.82	6.59
250	3.08	1.25	4.65	7.83
260	3.06	1.23	4.75	8.90
270	3.04	1.25	4.60	10.1
280	2.98	1.23	4.53	10.6
290	2.96	1.24	4.50	11.3
300	2.88	1.23	4.41	11.8
310	2.82	1.22	4.38	12.2
320	2.82	1.22	4.38	12.7
330	2.79	1.22	4.33	12.5
340	2.77	1.21	4.31	12.5
350	2.75	1.21	4.30	12.5
360	2.69	1.21	4.26	12.5
370	2.69	1.21	4.36	12.6
380	2.66	1.20	4.33	12.5
390	2.63	1.19	4.33	12.6
400	2.61	1.20	4.33	12.4
410	2.64	1.20	4.36	12.7
420	2.57	1.18	4.30	12.4
430	2.57	1.19	4.33	12.8
440	2.66	1.21	4.43	13.0
450	2.56	1.19	4.38	12.6
460	2.59	1.19	4.33	13.0
470	2.56	1.19	4.31	1.29
480	2.49	1.18	4.25	12.6
490	2.50	1.16	4.16	12.5

Table 3. (continued)

E_{el}/eV	$\sigma^{2+}/10^{-17}$ cm^2	$\sigma^{3+}/10^{-17}$ cm^2	$\sigma^{4+}/10^{-18}$ cm^2	$\sigma^{5+}/10^{-19}$ cm^2
500	2.49	1.19	4.30	12.3
510	2.47	1.18	4.20	12.3
520	2.46	1.18	4.14	12.4
530	2.39	1.14	4.14	11.9
540	2.40	1.16	4.08	12.1
550	2.36	1.13	4.09	11.9
560	2.34	1.13	4.01	11.7
570	2.32	1.11	3.89	11.4
580	2.29	1.10	3.86	11.1
590	2.29	1.08	3.87	11.1
600	2.24	1.08	3.91	10.9
610	2.27	1.08	3.82	10.9
620	2.20	1.04	3.74	10.9
630	2.16	1.04	3.70	10.3
640	2.15	1.02	3.67	10.4
650	2.14	1.01	3.69	10.4
660	2.10	1.00	3.57	10.1
670	2.09	1.00	3.45	9.71
680	2.05	0.98	3.40	9.66
690	2.02	0.96	3.42	9.41
700	1.97	0.95	3.40	9.50

sections the ion beam fractions will change remarkably with the target thickness. An interpretation of this dependence will lead to the initial beam fractions. For further information see Huber and Kahlert (1983).

Concerning the second method, the intensity ratio of ions produced by excitation and de-excitation processes is proportional to the ratio of the beam fractions. By solving coupled linear equations we obtain the beam fractions themselves.

In the case of Ne^{3+} the procedure was quite similar; spectra of Ne^{2+} ions produced in Ne^{3+}/Ne collisions have been used to obtain the metastable fractions. The corresponding results are shown in figures 4–7 and the data are listed in tables 4–7.

At electron energies just above threshold the beam composition is dominated by ions in the ground state. However, the corresponding fraction steeply decreases with increasing electron energy and finally approaches the statistical value. Analogously the number of ions in metastable states increases with electron energy; thus in Ne^{3+} about 80% of the ion beam is due to ions in low-lying metastable states. In the case of Ne^{2+} the ground-state fraction always remains dominant.

5. Conclusion

Partial cross sections for multiple ionisation by electron impact have been measured in neon, krypton and xenon, whereby charge states from 2 up to 8 are produced. The measured data agree well with results of other authors where available; however, there are significant differences from the results of Gaudin and Hagemann (1967) and Krishnakumar and Srivastava (1988) in particular at electron energies near threshold.

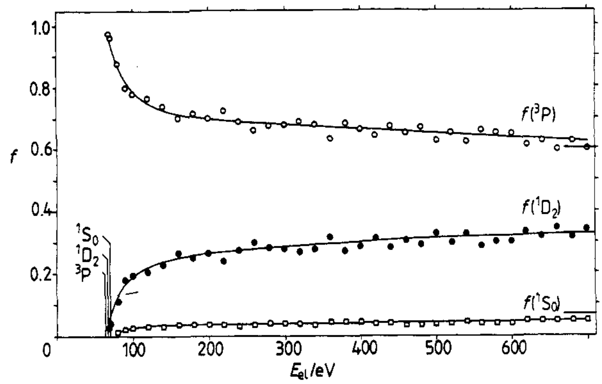

Figure 4. Beam fractions of Ne^{2+} ions plotted against electron energy. The vertical lines indicate the direct ionisation thresholds for the ground state ^3P and the two low-lying metastable states $^1D_2$ and $^1S_0$. The horizontal lines are computed with respect to a statistical distribution of the electronic states.

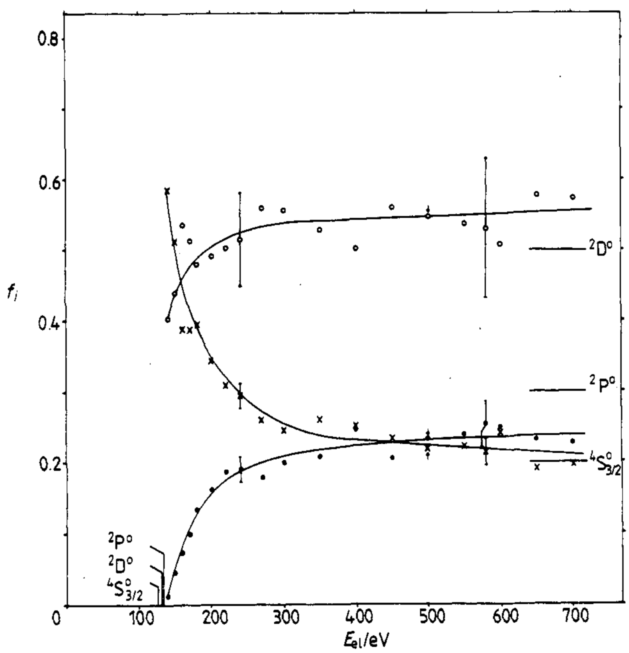

Figure 5. Beam fractions of Ne^{3+} ions plotted against electron energy. The total error is shown by the bars at 580 eV electron energy. The vertical lines indicate the direct ionisation thresholds for the ground state $^4S^o_{3/2}$ (×) and the two low-lying metastable states $^2D^o$ (○) and $^2P^o$ (●). The horizontal lines show the statistical distribution of the electronic states.

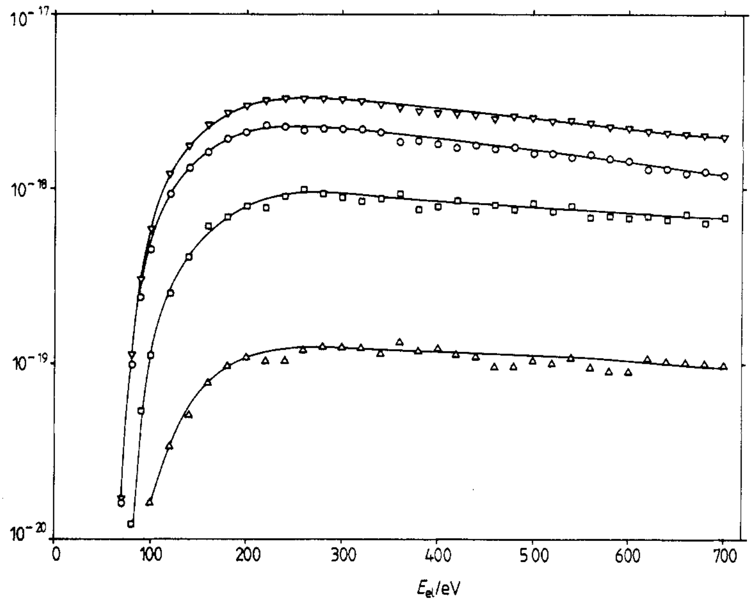

Figure 6. Partial and state-selective double ionisation cross sections for neon. The lines only guide the eye. ▽, unspecified; ○, ^3P; □, $^1D_2$; △, $^1S_0$.

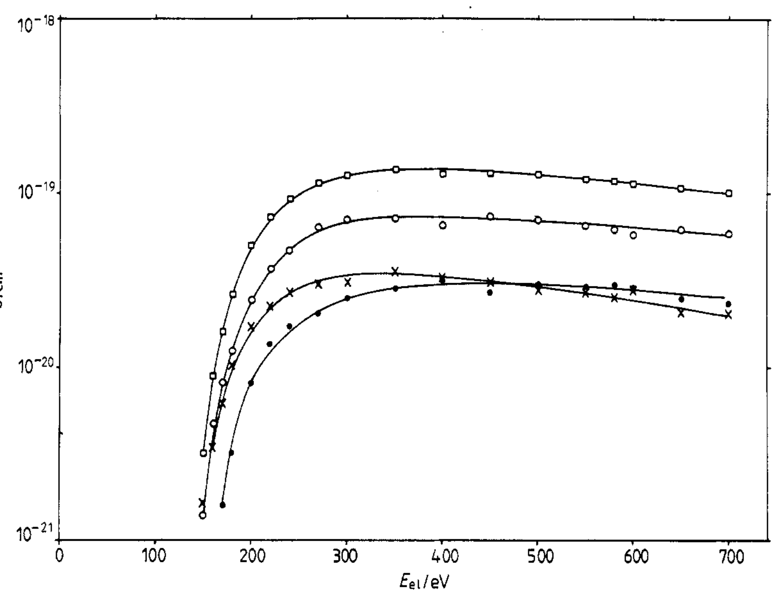

Figure 7. Partial and state-selective triple ionisation cross sections for neon. The lines only guide the eye. □, unspecified; ×, $^4S^o_{3/2}$; ○, $^2D^o$; ●, $^2P^o$.

Table 4. Beam fractions for Ne^{2+} ions produced by electron impact.

E_{el}/eV	$f(^3P)$	$f(^1D_2)$	$f(^1S_0)$
65	0.986	0.014	
68	0.976	0.024	
70	0.958	0.042	
80	0.881	0.109	0.010
90	0.800	0.179	0.021
100	0.778	0.194	0.028
120	0.766	0.205	0.028
140	0.741	0.230	0.029
160	0.702	0.264	0.034
180	0.713	0.251	0.036
200	0.700	0.264	0.036
220	0.725	0.242	0.033
240	0.693	0.275	0.032
260	0.662	0.301	0.037
280	0.675	0.287	0.038
300	0.682	0.279	0.039
320	0.693	0.268	0.039
340	0.682	0.281	0.037
360	0.635	0.318	0.046
380	0.684	0.273	0.043
400	0.664	0.290	0.046
420	0.643	0.315	0.042
440	0.673	0.285	0.042
460	0.653	0.310	0.037
480	0.669	0.294	0.037
500	0.629	0.329	0.042
520	0.655	0.303	0.042
540	0.625	0.330	0.045
560	0.667	0.291	0.041
580	0.655	0.305	0.040
600	0.652	0.307	0.041
620	0.613	0.335	0.051
640	0.630	0.320	0.050
660	0.600	0.350	0.050
680	0.632	0.318	0.050
700	0.604	0.346	0.050

Table 5. Partial and state-selective cross sections for the production of Ne^{2+} ions.

E_{el}/eV	$\sigma/10^{-18}$ cm^2	$\sigma(^3P)/10^{-18}$ cm^2	$\sigma(^1D_2)/10^{-19}$ cm^2	$\sigma(^1S_0)/10^{-19}$ cm^2
70	0.017	0.0163	0.007 17	
80	0.112	0.0987	0.122	0.0111
90	0.300	0.240	0.538	0.0624
100	0.584	0.454	1.13	0.162
120	1.21	0.927	2.48	0.341
140	1.77	1.31	4.06	0.510
160	2.30	1.61	6.07	0.780
180	2.71	1.93	6.80	0.973
200	2.99	2.09	7.89	1.09
220	3.18	2.30	7.71	1.04
240	3.26	2.26	8.97	1.04
260	3.25	2.15	9.79	1.20
280	3.24	2.19	9.30	1.24
300	3.20	2.18	8.93	1.25
320	3.14	2.17	8.42	1.23
340	3.07	2.09	8.63	1.14
360	2.92	1.86	9.29	1.35
380	2.78	1.90	7.58	1.20
400	2.71	1.80	7.87	1.24
420	2.70	1.74	8.51	1.13
440	2.64	1.78	7.51	1.11
460	2.62	1.71	8.12	0.964
480	2.59	1.73	7.61	0.966
500	2.53	1.59	8.33	1.06
520	2.45	1.61	7.42	1.02
540	2.43	1.52	8.01	1.05
560	2.35	1.57	6.84	0.971
580	2.29	1.50	6.98	0.918
600	2.22	1.45	6.82	0.904
620	2.12	1.30	7.11	1.08
640	2.08	1.31	6.65	1.04
660	2.05	1.23	7.17	1.04
680	2.01	1.27	6.40	1.01
700	1.99	1.20	6.89	0.991

Table 6. Beam fractions for Ne^{3+} ions produced by electron impact.

E_{el}/eV	$f(^4S^o_{3/2})$	$f(^2D^o)$	$f(^2P^o)$
140	0.585	0.403	0.012
150	0.513	0.440	0.047
160	0.389	0.536	0.075
170	0.388	0.512	0.100
180	0.396	0.480	0.124
200	0.345	0.492	0.163
220	0.310	0.503	0.187
240	0.295	0.515	0.191
270	0.261	0.559	0.180
300	0.246	0.557	0.198
350	0.261	0.529	0.209
400	0.251	0.502	0.247
450	0.234	0.560	0.206
500	0.219	0.547	0.234
550	0.223	0.537	0.240
580	0.215	0.531	0.254
600	0.242	0.508	0.250
650	0.191	0.578	0.232
700	0.197	0.575	0.228

Table 7. Partial and state-selective cross sections for the production of Ne^{3+} ions.

E_{el}/eV	$\sigma/10^{-19}$ cm^2	$\sigma(^4S^o_{3/2})/10^{-20}$ cm^2	$\sigma(^2D^o)/10^{-20}$ cm^2	$\sigma(^2P^o)/10^{-20}$ cm^2
140	0.008 09	0.0473	0.0326	0.001 04
150	0.032 1	0.165	0.141	0.015 2
160	0.088 6	0.345	0.475	0.065 9
170	0.160	0.620	0.820	0.160
180	0.261	1.03	1.25	0.322
200	0.501	1.73	2.46	0.818
220	0.733	2.27	3.69	1.38
240	0.915	2.70	4.71	1.74
270	1.15	3.00	6.43	2.07
300	1.27	3.12	7.07	2.51
350	1.37	3.58	7.25	2.87
400	1.31	3.29	6.57	3.24
450	1.32	3.09	7.39	2.72
500	1.29	2.83	7.06	3.02
550	1.22	2.71	6.55	2.93
580	1.19	2.55	6.32	3.03
600	1.15	2.78	5.84	2.88
650	1.09	2.08	6.29	2.52
700	1.03	2.03	5.92	2.35

In the case of double and triple ionisation of xenon, structures in the cross sections are explained by inner-shell contributions.

State-selective cross sections yield information on the ion beam composition emphasising a strong contamination of Ne^{2+} and Ne^{3+} beams with ions in metastable states provided multiply charged ions are produced by single electron impact.

Acknowledgments

The financial support by the Deutsche Forschungsgemeinschaft is gratefully acknowledged.

References

Gaudin A and Hagemann R 1967 *J. Chem. Phys.* **64** 1209
Huber B A 1987 *Comment At. Mol. Phys.* **21** 15
Huber B A and Kahlert H J 1983 *J. Phys. B: At. Mol. Phys.* **16** 4655
—— 1984 *J. Phys. B: At. Mol. Phys.* **17** L69
Kobayashi N, Nakamura T and Kaneko Y 1983 *J. Phys. Soc. Japan* **52** 2684
Koslowski H R, Binder J, Huber B A and Wiesemann K 1987 *J. Phys. B: At. Mol. Phys.* **20** 5903
Krishnakumar E and Srivastava S K 1988 *J. Phys. B: At. Mol. Opt. Phys.* **21** 1055
Nagy P, Skutlartz A and Schmidt V 1980 *J. Phys. B: At. Mol. Phys.* **13** 1249
Rapp D and Englander-Golden P 1965 *J. Chem. Phys.* **43** 1464
Schram B L 1966 *Physica* **32** 197
Schram B L, Boerboom A J H and Kistemaker J 1966 *Physica* **32** 185
Stephan K, Helm H and Märk T D 1980 *J. Chem. Phys.* **73** 3763
Stephan K and Märk T D 1984 *J. Chem. Phys.* **81** 3116
Stuber F A 1965 *J. Chem. Phys.* **42** 2639
Wetzel R C, Baiocchi F A, Hayes T R and Freund R S 1987 *Phys. Rev.* A **35** 559
Wiesemann K, Puerta J and Huber B A 1987 *J. Phys. B: At. Mol. Phys.* **20** 587